

1 **Editing of the urease gene by CRISPR-Cas in the diatom *Thalassiosira pseudonana***

2

3 Amanda Hopes¹, Vladimir Nekrasov², Sophien Kamoun² & Thomas Mock^{1*}

4

5 ¹ School of Environmental Science, University of East Anglia, Norwich Research Park, NR4 7TJ,
6 Norwich, UK.

7 ² The Sainsbury Laboratory, Norwich Research Park, NR4 7UH, Norwich, UK

8 * Corresponding author email: t.mock@uea.ac.uk

9

10 **Abstract**

11 **Background:** CRISPR-Cas is a recent and powerful edition to the molecular toolbox which allows
12 programmable genome editing. It has been used to modify genes in a wide variety of organisms, but
13 only two alga to date. Here we present a methodology to edit the genome of *T. pseudonana*, a
14 model centric diatom with both ecological significance and high biotechnological potential, using
15 CRISPR-Cas.

16 **Results:** A single construct wa assembled using Golden Gate cloning. Two sgRNAs were used to
17 introduce a precise 37nt deletion early in the coding region of the urease gene. A high percentage of
18 bi-allelic mutations ($\leq 61.5\%$) were observed in clones with the CRISPR-Cas construct. Growth of bi-
19 allelic mutants in urea led to a significant reduction in growth rate and cell size compared to growth
20 in nitrate.

21 **Conclusions:** CRISPR-Cas can precisely and efficiently edit the genome of *T. pseudonana*. The use of
22 Golden Gate cloning to assemble CRISPR-Cas constructs gives additional flexibility to the CRISPR-Cas
23 method and facilitates modifications to target alternative genes or species.

24

25 **Keywords:** CRISPR-Cas, diatom, genome editing, urease, Golden Gate, *Thalassiosira pseudonana*

26

27

28 **Background**

29 Diatoms are ecologically important microalgae with high biotechnological potential. Since their
30 appearance about 240 million years ago [1], they have spread and diversified to occupy a wide range
31 of niches across both marine and freshwater habitats. Diatom genomes have been shaped by
32 secondary endosymbiosis and horizontal gene transfer resulting in genes derived from heterotrophic
33 hosts, autotrophic endosymbionts and bacteria [2, 3]. They play a key role in carbon cycling [4], the
34 food chain, oil deposition and account for about 20% of the world's annual primary production [5,
35 6]. However, they are perhaps best known for their intricate silica frustules which give diatoms a
36 range of ecological advantages and play a key role for carbon sequestration and silica deposition.

37 Several aspects of diatom physiology including the silica frustule, lipid storage and photosynthesis
38 are being applied to biotechnology. Areas of high interest include nanotechnology [7], drug delivery
39 [8], biofuels [9], solar capture [10] and bioactive compounds [11].

40 Given the ecological importance of diatoms and their applications for biotechnology, it is pivotal that
41 the necessary tools are available to study and manipulate them at a molecular level. This includes
42 the ability to replace, tag, edit and impair genes. A recent addition to the genetic tool box, CRISPR-
43 Cas, allows double strand breaks (DSBs) to be introduced at specific target sequences. This adapted
44 mechanism, used by bacteria and archaea in nature as a defence system against viruses, facilitates
45 knock-out by the introduction of mutations through repair by error prone non-homologous end
46 joining (NHEJ) or homologous recombination (HR). This requires both a Cas9 to cut the DNA and a
47 sgRNA to guide it to a specific sequence. Further information on the history and application of
48 CRISPR-Cas can be found in several excellent reviews [12–14]. Zinc-finger nucleases (ZFNs),
49 meganucleases and transcription activator-like effector nucleases (TALENs) have also been used to
50 induce double strand breaks. TALENs and CRISPR-Cas both bring flexibility and specificity to gene
51 editing, however CRISPR-Cas is also cheap, efficient and easily adapted to different sequences by
52 simply changing the 20nt guide sequence in the sgRNA.

53 So far, within the diverse group of algae, the diploid, pennate diatom *Phaeodactylum tricoratum*
54 [15] and the haploid, green alga *Chlamydomonas reinhardtii* [16] have been subject to gene editing
55 by CRISPR-Cas. NHEJ and HR have been used to repair DSBs following CRISPR-Cas or TALENs in *P.*
56 *tricoratum*, introducing mutations into a nuclear coded chloroplast signal recognition particle [15],
57 the urease gene [17] and several genes associated with lipid metabolism [18]. *Thalassiosira*
58 *pseudonana* is a logical choice for CRISPR-Cas development. It is a model centric diatom with a
59 sequenced genome (first eukaryotic marine phytoplankton to be sequenced [2]) and well-
60 established transformation systems [19, 20]. The genus has multiple biotechnology applications [8,
61 21, 22], and although gene silencing has been established, a method to easily and efficiently knock-
62 out and edit genes and the entire genome would be highly advantageous. The genus *Thalassiosira* is
63 among the top 10 genera of diatoms in the World's Ocean in terms of ribotype (V9 of 18S) diversity
64 and abundance [23] and the species *T. pseudonana* is a model for understanding the mechanisms
65 behind silicification [24–26].

66 Golden Gate cloning can add further flexibility to CRISPR-Cas methods as demonstrated in higher
67 plants [27]. As a modular cloning system it allows different modules, including the sgRNA, to be
68 easily interchanged or added [28]. As a result, new constructs can be made quickly, cheaply and
69 efficiently for new or multiple targets. This extends to any aspect of the construct, including
70 promoters, Cas9 variants and their nuclear localisation signals (NLS). As a result, construct
71 alterations such as replacing constitutive promoters for inducible ones, exchanging the wildtype

72 Cas9 for a Cas9 nickase or changing the localisation signal to target other organelles can be easily
73 carried out.

74 An increasing range of software tools are available for CRISPR-Cas, including programs that facilitate
75 sgRNA target searches in a genetic locus of interest, estimate efficiencies of sgRNAs [29] and
76 perform off-target predictions.

77 While off-target prediction tools tend to be species specific, there are tools that accept requests for
78 a genome to be added to the list, or allow for a genome to be directly uploaded [30, 31]. The latter is
79 particularly useful for less studied organisms, such as diatoms. The ability to combine several
80 different aspects of sgRNA design can help to make an informed decision when choosing target sites
81 for gene editing.

82 Our paper represents a proof of concept to demonstrate the feasibility of gene editing in the model
83 diatom *T. pseudonana* using two sgRNAs to induce a precise deletion in the urease gene. Methods
84 combine a flexible Golden Gate cloning approach with sgRNA design, which draws on several
85 available online tools. This takes into account multiple factors, such as position within the gene in
86 terms of both early protein disruption and presence in the coding region, DNA cutting efficiency and
87 presence of restriction enzyme sites at the cut site. The latter, in combination with inducing a large
88 deletion by targeting with two sgRNAs, allows easy screening of mutants through either the
89 restriction enzyme site loss assay [32] or the PCR band-shift assay [33], respectively.

90

91 **Method**

92 **Strains and growth conditions**

93 *Thalassiosira pseudonana* (CCMP 1335) was grown in 24h light (100-140 μ E) at 20°C in half salinity
94 Aquil synthetic seawater [34]. For routine growth, a 1mM nitrate concentration was used.

95 **5'RACE U6 promoter**

96 To identify the U6 small nuclear RNA (snRNA) in *T. pseudonana*, an NCBI blastn search was
97 performed on the genome against the central conserved region of the U6 sequence. Two potential
98 guanine (G) start sites were found downstream of a TATA box in the promoter. To identify the start
99 site of the U6 snRNA and empirically determine the end of the promoter, 5' RACE was carried out as
100 follows: 400ml of culture was grown to exponential phase (1×10^6 cells ml⁻¹) and harvested. Small
101 RNAs were extracted and enriched using a miRNeasy kit (Qiagen). 5' template switching oligo RACE
102 was performed according to Pinto and Lindblad [35]. For oligos used see Table 1 (ref. numbers 1-3).
103 RACE products were sequenced and results aligned to the genome to determine the end of the
104 promoter.

105

106 **Plasmid construction using Golden Gate cloning**

107 Golden Gate cloning was carried out according to Weber et al. [28] and Belhaj et al. [33]. Bsal and
108 Bpil sites were removed in a so-called "domestication" procedure using a Q5 site-directed
109 mutagenesis (SDM) kit (NEB). For oligos used in SDM see Table 1 (ref. numbers 17-20). Bsal sites and
110 specific 4nt overhangs for Level 1 (L1) assembly were added through PCR primers (Table 1). Plasmid
111 DNA was extracted using a Promega mini-prep kit.

112 Golden Gate reactions

113 Golden Gate reactions for L1 and Level 2 (L2) assembly were carried out using the method specified
114 in Weber et al. [28]. Forty fmol of each component was included in a 20 μ l reaction with 10 units of
115 Bsal or Bpil and 10 units of T4 DNA ligase in 1x ligation buffer. The reaction was incubated at 37°C for

116 5 hours, 50°C for 5 minutes and 80°C for 10 minutes. Five µl of the reaction was transformed into
117 50µl of NEB 5-alpha chemically competent *E. coli*.

118 Level 0 assembly

119 The endogenous FCP promoter and terminator were amplified with GoTaq flexi (Promega) from
120 domesticated pTpFCP/NAT [19] and the U6 promoter from gDNA (extracted with an Easy-DNA gDNA
121 purification kit (Thermo Fisher)). Both promoters are associated with high expression levels. The U6
122 promoter was amplified from the position -470 to -1 (the end of the promoter), cutting off a Bpil site
123 and removing the need for additional SDM. For oligos, see Table 1 (ref. numbers 6-7 and 10-13).

124 Products were cloned into a pCR8/GW/TOPO vector (Thermo Fisher).

125 Domesticated human codon bias Cas9 from *Streptococcus pyogenes* with an N-terminal SV40 NLS
126 and a C-terminal YFP tag was PCR-amplified using Phusion DNA polymerase (NEB) and L1 Cas9:YFP
127 plasmid as a template. The PCR product was purified with a GFX PCR DNA and gel purification kit (GE
128 Healthcare) and incubated for 20 minutes with Taq to add adenine overhangs before cloning directly
129 into a pCR8/GW/TOPO vector. For oligos, see Table 1 (ref. numbers 8-9).

130 Level 1 assembly

131 The FCP:NAT cassette was PCR-amplified using Phusion polymerase and the domesticated
132 pTpFCP/NAT as a template, purified and inserted into a L1 pICH47732 destination vector. FCP
133 promoter, Cas9 and FCP terminator L0 modules were assembled into L1 pICH47742. For oligos, see
134 Table 1 (ref. numbers 4-5).

135 The sgRNA scaffold was amplified from pICH86966_AtU6p_sgRNA_NbPDS [32] with sgRNA guide
136 sequences integrated through the forward primers. Together with the L0 U6 promoter,
137 sgRNA_Urease 1 and sgRNA_Urease 2 were assembled into L1 destination vectors pICH47751 and
138 pICH47761, respectively. For oligos, see Table 1 (ref. numbers 14-16).

139 Level 2 assembly

140 L1 modules pICH47732:FCP:NAT, pICH47742:FCP:Cas9YFP, pICH47751:U6:sgRNA_Urease 1,
141 pICH47761:U6:sgRNA_Urease 2 and the L4E linker pICH41780 were assembled into the L2
142 destination vector pAGM4723. Constructs were screened by digestion with EcoRV and sequenced.
143 For oligos used in sequencing, see Table 1 (ref. numbers 27-35). See Figure 1 for an overview of the
144 Golden Gate assembly procedure and the final construct.

145

146 **sgRNA design for the urease gene knockout**

147 Two sgRNAs were designed to cut 37nt apart early in the coding region of the urease gene (JGI ID
148 30193) to induce a deletion and frame-shift. Several programmes, explained below, were used to
149 collect data and make an informed decision on sgRNA choice. Excel was used to combine, process
150 and compare data.

151 Selecting CRISPR-Cas targets and estimating on-target score

152 Twenty bp targets with an NGG PAM were identified and scored for on-target efficiency using the
153 Broad Institute sgRNA design programme (www.broadinstitute.org/rnai/public/analysis-tools/sgrna-design), which utilises the Doench et al. [29] on-target scoring algorithm calculated from >1800
154 empirically tested sgRNAs.

156 Determining cut positions and cross referencing to restriction recognition sites

157 All restriction sites and their positions within the urease gene were identified using the Emboss
158 restriction tool (<http://emboss.bioinformatics.nl/>). As the Broad Institute sgRNA design programme
159 does not give the location of CRISPR-Cas targets within a gene, this was determined using Primer
160 map (http://www.bioinformatics.org/sms2/primer_map.html [36]). The cut site position (3nt
161 upstream of the start of the PAM sequence) was calculated for each sgRNA depending on sense or
162 anti-sense strand placement. All predicted CRISPR-Cas cut sites were cross-referenced to restriction
163 recognition sites.

164 Reverse complement of antisense strand CRISPR-Cas targets

165 The reverse complement (RC) was found for each CRISPR-Cas target using the programme:
166 http://www.bioinformatics.org/sms2/rev_comp.html [36]. In the final spreadsheet (Supplementary
167 Figure 1), if a target was located on the anti-sense strand, the RC was shown for the 'sense strand
168 sequence' column. This allows the sgRNA to be easily searched within the original gene sequence.

169 Determine position of CRISPR-Cas cut sites in relation to coding region

170 An array was made with start and end positions for each exon/intron. Cut site positions were
171 compared to exon/intron ranges and the relevant exon/intron returned if the data overlapped.
172 The final spreadsheet gives data on CRISPR-Cas target sequences and their sense sequence (if
173 located on the antisense strand), location of target (relative to the sense strand), predicted CRISPR-
174 Cas cut site, first nucleotide of the target, PAM sequence, location (i.e. exon, intron), strand, sgRNA
175 score and restriction recognition sites overlapping the cut site. The table (Supplementary Figure 1)
176 was sorted to prioritise sgRNAs by starting base prioritising guanine, sgRNA score, position within
177 the gene and interaction with restriction recognition sites.

178 Predicting off-targets

179 The full 20nt target sequences and their 3' 12nt seed sequences were subjected to a nucleotide
180 BLAST search against the *T. pseudonana* genome. Resulting homologous sequences were checked
181 for presence of an adjacent NGG PAM sequence at the 3' end. The 8nt sequence outside of the seed
182 sequence was manually checked for complementarity to the target sequence. In order for a site to
183 be considered a potential off-target the seed sequence had to match, a PAM had to be present at
184 the 3' end of the sequence and a maximum of three mismatches between the target and sequences
185 from the blast search were allowed outside of the seed sequence.

186 Off-targets were also checked using the EuPaGDT program [31], which checks for up to 5
187 mismatches in the 20nt target sequence and the CasOT program [30], which uses flexible
188 parameters for identifying off-target sequences. Parameters were set to check for an NGG PAM,
189 complete complementarity within the 12nt seed sequence and up to 3 mismatches outside of the
190 seed region.

191

192 **Transformation and selection**

193 Using the Poulsen et al. [19] method, transformations were carried out in triplicate with the CRISPR-
194 Cas construct, pTpfcp/nat (positive control) and water (negative control). Five x 10⁷ cells in
195 exponential phase were used per shot with a rupture disc of 1350psi and a 7cm flight distance.
196 Following transformation, cells were rinsed into 25ml of media and left to recover for 24 hours
197 under standard growth conditions. Cells were counted using a Coulter counter (Beckman) and 2.5 x
198 10⁷ cells from each transformation were spread onto 5, ½ salinity Aquil 0.8% agar plates (5 x 10⁶
199 cells/ plate) with 100µg ml⁻¹ nourseothricin. Plates were incubated under standard conditions for
200 two weeks. Remaining sample was diluted to 1 x 10⁶ cell ml⁻¹ in media and supplemented with
201 nourseothricin to final a concentration of 100µg ml⁻¹ for liquid selection. Liquid selection cultures
202 were maintained under standard growth conditions with 100µg ml⁻¹ nourseothricin. Colonies were
203 picked and transferred to 20µl of media. Ten µl from each colony was transferred to 1ml of selective
204 media for further growth. The remaining sample was used in screening.

205 To isolate sub-clones from colonies which screened positive for mutations, 100µl of cells at
206 exponential phase were streaked onto ½ salinity Aquil 0.8% agar plates with 100µg ml⁻¹
207 nourseothricin.

208 **Screening clones and cultures**

209 Ten µl from each colony or culture from liquid selection, was spun down and supernatant removed.
210 Cells were re-suspended in 20µl of lysis buffer (10% Triton X-100, 20mM Tris-HCl pH8, 10mM EDTA),

211 kept on ice for 15 minutes then incubated at 95°C for 10 minutes. One μ l of lysate was used in Taq
212 PCR to amplify the CRISPR-Cas targeted fragment of the urease gene. Clones were also screened for
213 Cas9 and NAT. For PCR primers, see Table 1 (ref. numbers 21-26). PCR products were run on an
214 agarose gel to check for the lower MW band associated with a double-cut deletion in the urease
215 gene and for the presence of Cas9 and NAT. Urease PCR products were also digested with BsaI and
216 HpaII to determine if the restriction recognition sites, which overlap the cut sites, had been mutated.
217 PCR products were sent for sequencing to confirm mutations.

218 **Growth experiments**

219 Knockout and wild-type (WT) cultures were nitrate depleted by growing cells in nitrate free media
220 until cell division stopped and quantum yield of photosynthesis (Fv/Fm measured on the Phyto-
221 PAM-ED) dropped below 0.2. Cultures were then transferred in triplicate at a final concentration of
222 2.5×10^4 cells ml^{-1} into 25ml of media with either 1mM sodium nitrate or 0.5mM urea. Cell count
223 and mean cell size were measured once a day using a Coulter counter. Fv/Fm measurements were
224 also taken daily. Growth rates were calculated using $\mu = \frac{\ln_2 - \ln_1}{T_2 - T_1}$, where T is a time point
225 corresponding to exponential growth and \ln is the natural log of cell counts ml^{-1} . Analysis of variance
226 with Tukey's pairwise comparison was used to compare both growth rates and cell size at the end of
227 exponential phase between samples.

228

229 **Results and discussion**

230 **sgRNA design**

231 The two CRISPR-Cas targets with the highest on target scores (0.5 and 0.79), containing a predicted
232 cut site over a restriction site and occurring early in the coding region, were chosen. sgRNAs were
233 designed to cut 37nt apart at positions 138 and 175 within the urease gene. Both targets started
234 with a G for polymerase III transcription (Figure 2). No off-target sites were predicted for sgRNAs
235 designed for either of the two CRISPR-Cas target sequences.

236

237 **Constructing the CRISPR-Cas plasmid using the Golden Gate cloning method**

238 A single CRISPR-Cas construct was made using Golden Gate cloning (Figure 1). The construct
239 included the NAT selectable marker and Cas9:YFP driven by an endogenous FCP promoter for high
240 expression and two U6 promoter-driven sgRNAs. RNA polymerase III U6 promoters are a popular
241 choice for expression of sgRNAs in CRISPR-Cas [15, 27, 37–39]. RACE products showed that the U6
242 promoter ended 23nt after the TATA box. As a standardised, efficient, modular system, Golden Gate
243 cloning gives a high level of flexibility to the CRISPR-Cas method and bypasses the need for co-
244 transformation as it enables assembly of multiple expression units, such as Cas9 and sgRNAs, into a
245 single vector backbone. Multiple sgRNA modules can be incorporated into the construct to target
246 several genes or whole pathways. In human cells, up to 7 sgRNAs have been successfully assembled
247 and expressed from a single construct created using the Golden Gate cloning method [39]. Golden
248 Gate has also proved successful for building constructs for genome editing in higher plants using
249 both TALENs [41] and CRISPR-Cas [33, 37].

250 In this study, only the promoters and target sequences are specific to *T. pseudonana*, which
251 demonstrates how simple it can be to apply this method to a new species using the Golden Gate
252 system. The *S. pyrogenes* Cas9 with a human codon bias, shown previously to work in higher plants
253 [32, 33, 37], carries a SV40 NLS, which follows a canonical sequence found throughout eukaryotes,
254 including *T. pseudonana*.

255 The long term effects from off-target mutations introduced through CRISPR-Cas are currently
256 unknown, therefore it may be advantageous for future work to remove CRISPR-Cas constructs from
257 mutants. Adding a yeast CEN6-ARSH4-HIS3 sequence to plasmids allows autonomous replication in
258 diatoms and expression of genes without random integration into the genome [20]. Furthermore,
259 removing selection leads to plasmids being discarded. By expressing CRISPR-Cas genes and selective
260 markers on a removable episome, mutations could be introduced without integration of the
261 plasmid. CRISPR-Cas constructs could then be expelled by removing selection. As well as
262 considerations for long term off-target effects, this could also be advantageous for studies and
263 applications which are sensitive to the presence of transgenes.

264 **Selecting and screening for mutations in the urease gene**

265 The transformation efficiency with the CRISPR-Cas construct was on average 41.5 colonies μg^{-1}
266 plasmid (13.35-66.65 colonies μg^{-1} plasmid). Thirty three colonies were screened by PCR and
267 sequencing of the targeted urease gene fragment.

268 Four colonies showed mutations in the urease gene. All colonies screened positive for NAT but only
269 the four colonies with mutations screened positive for Cas9, suggesting that once the Cas9 and
270 sgRNAs are present there is a high chance of inducing mutations in the target gene. The lack of Cas9,
271 which accounts for a third of the construct, in the majority of colonies was potentially caused by
272 shearing of the plasmid during microparticle bombardment [38] from either mechanical force or
273 chemical breakdown [42].

274 Of the four primary colonies which screened positive for mutations (Figure 2), one (M4) showed a
275 single band with a 37nt deletion between the two sgRNA cut sites which suggests that both copies of
276 the urease gene contain the deletion giving a bi-allelic mutant. Two colonies (M2 and M3) produced
277 two bands following PCR: a WT higher MW band and a lower MW band with the 37nt deletion,
278 confirmed by sequencing (Figure 2). The fourth colony (M1) showed a single band associated with
279 the WT urease, however sequencing showed two products: a WT urease and a mutant urease with a
280 4nt deletion at the first sgRNA cut site. A mixture of PCR products may be due to a mono-allelic
281 mutation, in which one allele is WT and the other displays a mutation. It can also be due to colony
282 mosaicism where a colony contains a mixture of cells with WT and mutant alleles due to mutations
283 occurring after transformed cells have started to divide. Both mono-allelic mutants and mosaic
284 colonies have been observed in *P. tricornutum* [15, 18].

285 To determine if the colonies were mosaic or mono-allelic, cells from mutant clones producing mixed
286 PCR products were spread onto selective plates to isolate single sub-clones. Thirty four sub-clones
287 from each clone were screened by PCR (a few examples are presented in Figure 2). Two clones (M2
288 and M3) were mosaic with a mixture of sub-clones showing either a single band corresponding to
289 the expected deletion (61.5% and 25%, respectively), two bands associated with the WT and
290 expected deletion (25.5% and 28.1%, respectively) or a single band corresponding to the WT urease
291 fragment (13% and 46.9% respectively). For each of the two clones PCR amplicons from three
292 putative bi-allelic sub-clones were sequenced (Figure 2). Four out of six (M2_9, M2_10, M3_10 and
293 M3_11) showed the expected 37nt 'clean' deletion without any additional mutations. Precise
294 deletions, such as this, using 2 sgRNAs have previously been generated with high efficiency [37, 43],
295 and allow a large degree of control over the mutation. Two of the sub-clones (M3_9 and M2_12)
296 showed one allele with the expected 37nt deletion and the other with an additional deletion at the
297 2nd sgRNA cut site. In addition, M2_12 showed a C->G SNP within the sgRNA1 target site. Sub-clones
298 derived from the M1 clone showed WT and 4nt deletion PCR amplicons as seen in the original clone,
299 suggesting that this clone may have a mono-allelic mutation.

300 Using CRISPR-Cas with one sgRNA can introduce a variety of indels into a locus of interest via the
301 error-prone NHEJ DNA repair mechanism [15]. Cas9 preferentially cuts DNA three nucleotides
302 upstream of the PAM sequence in the seed region [44] and the NHEJ mechanism either repairs a
303 double strand break perfectly or indels are introduced. If cut sites are not cleaved at the same time,
304 when using two sgRNAs, mutations at each site rather than removal of the fragment in between
305 target sites may occur [37]. In this study, however, we report a high occurrence of bi-allelic mutants
306 with precise deletions between the CRISPR-Cas cut sites, suggesting that the Cas9/sgRNA complex is
307 cutting efficiently and DNA ends tend to be repaired perfectly. This allows control over the
308 introduced mutations and gives the chance to avoid introducing in-frame indels.

309 Restriction digest (results not shown) and sequencing (Figure 2) demonstrated loss off the BclI site
310 in all knock-out clones and HpaII in M2_12 and M1 as a deletion downstream of the cut site is
311 required to remove the HpaII site. This demonstrates that restriction screening can be a valuable
312 tool, however in this case screening for a deletion based band shift by PCR was an efficient way of
313 identifying bi-allelic mutants especially given the limited sgRNA/restriction site interactions available
314 for this gene.

315 As well as clones from plate selection, one culture from liquid selection (LM1; population of cells
316 transferred to liquid selective media after transformation), showed a single band associated with the
317 bi-allelic 37nt deletion following PCR. This was confirmed by sequencing (Figure 2). PCR screening
318 following growth of LM1 in urea showed only the lower MW band product (results not shown),
319 giving further evidence for a bi-allelic mutation from a population of cells. As small volumes of cells
320 are transferred to fresh media when passaging this may have isolated bi-allelic mutants.

321 **Growth experiments with mutants**

322 Urease catalyses the breakdown of urea to ammonia allowing it to be used as a source of nitrogen
323 [45]. Sub-clones from different cell-lines with 37 or 38nt deletions were tested for knock-out of the
324 urease gene by looking for a lack of growth when supplemented with urea as the sole nitrogen
325 source.

326 Cells were nitrogen starved and then transferred to media with either nitrate or urea. Cell counts,
327 cells size and Fv/Fm were measured daily for 7 days. Negative controls to account for any
328 background nitrate in the media were also run in which no nitrate or urea was added for WT
329 cultures.

330 Four putative bi-allelic mutants (LM1, M4, M2_10 and M3_9) were tested along with WT and the
331 mono-allelic M1_10 over two growth curve experiments. Both LM1 from liquid selection ($p=0.0029$)
332 and the sub-clone M3_9 ($p=0.0000001$) showed a significant decrease in growth rate in urea
333 compared to nitrate (Figure 3) as well as a significant 13-18% decrease in cell size (Figure 4;
334 $p=0.0029$ and $p=0$, respectively). The latter was also apparent with light microscopy (results not
335 shown). Mutants in urea could be easily discerned even without cell counts, as cultures appeared
336 much paler in colour. M4 did not show a difference in growth rate but did show a significant
337 decrease in cell size ($p=0.038$). The mono-allelic mutant M1_10, displayed higher growth in urea and
338 similar growth to the WT control (Figure 3). This correlates with results from Weyman et al. [17]
339 which showed that despite a reduced protein concentration, a mono-allelic urease knock-out was
340 able to grow in urea. M2_10 which screened as a bi-allelic mutant prior to growth experiments
341 showed a smaller but still significant decrease in growth rate ($p=0.0014$) (Figure 3) and cell size
342 ($p=0.0039$) (Figure 4). PCR screening of the urease gene following growth in nitrate and urea showed
343 the expected bi-allelic mutation for LM1, M3_9 and M4, however M2_10 also showed a faint WT
344 band in nitrate and a strong WT band in urea (Figure 5). This suggests that M2_10 was mosaic, with
345 cells containing a functional urease out-competing those with a mutant urease. Given that only a

346 faint WT band was present after growth in nitrate this suggests that the majority of the cells from
347 the sub clone contained the mutant urease, initially accounting for the majority of growth and
348 resulting in a lower but still significant decrease in growth rate.

349 Knock-out of the urease gene in the diatom *P. tricornutum* prevents growth in urea [17]. Urease
350 mutants in this study still grew in urea but with a lower growth rate and reduced cell-size,
351 characteristics which are associated with nitrogen limitation in diatoms [46, 47] rather than nitrogen
352 starvation. Mutant cell-lines in urea grew to the same density as the same cell-lines in nitrate, but at
353 a lower rate (Figure 3). As nitrogen is an essential nutrient for growth, this suggests that mutant cells
354 in urea still have access to nitrogen, but lower growth rates and cell-size indicates that nitrogen may
355 not be as readily available compared to cells grown with nitrate. Controls in nitrogen free media
356 showed very little growth which suggests that growth of mutants in urea was not due to residual
357 nitrate in the culture. It is unlikely that random integration of the CRISPR-Cas plasmid is responsible
358 for reduced growth rate in mutants as all four individual mutant cell-lines display increased growth
359 rates when grown in nitrate. Therefore it seems likely that impaired growth of urease mutants in
360 urea is due to a reduction in function of the urease gene.

361 There are a few possible reasons why a mutation in the urease gene appears to lead to nitrogen
362 limitation rather than nitrogen starvation as seen in *P. tricornutum*. Cells may be able to access
363 nitrogen from another source, separate to the breakdown of urea via urease. Some algae have an
364 alternative pathway for breakdown of urea but this has only been found in Chlorophyceae [48] and
365 blast searches show no evidence of urea carboxylase or allophanate hydroxylase, the enzymes
366 involved in this pathway, in *T. pseudonana*.

367 The urease gene may still be active but with lower functionality. In *T. pseudonana* urease is
368 modelled to be 807 amino acids. Urease consists of multimers of three sub-units: gamma, beta and
369 alpha, which in TP are translated as one protein. The alpha sub-unit contains the active site which
370 catalyses the breakdown of urea to ammonia [45]. The gamma subunit has no known enzymatic
371 function [49] but may play a role in quaternary structure and stability [45, 50].

372 Translations of urease sequences with both 37 and 38nt deletions show frame shifts and early stop
373 codons after the deletion in the gamma sub-unit, leading to major disruption of the gamma sub-unit,
374 nonsense down-stream and short products of 24 or 44 amino acid residues (Figure 6). Since all
375 mono-clonal bi-allelic mutants tested for growth in urea had either two alleles with a 37nt deletion
376 or both a 37 and 38nt deletion, it was predicted that the urease gene would no longer be functional.
377 However, several mechanisms exist in eukaryotes which can allow translation of the protein from
378 start codons later in the coding region. These include leaky initiation, re-initiation of ribosomes and
379 internal ribosome entry sites (IRES) [51]. IRES have been shown to become active in yeast following
380 amino acid starvation [51]. If an in-frame translation can occur after the deletion at an IRES or via a
381 mechanism such as re-initiation then the active site located in the alpha-subunit could still be
382 present. The first in-frame ATG after the deletion would start translation of the protein just before
383 the beta sub-unit, leading to an N-terminal truncated protein without the gamma sub-unit but with
384 both the beta and alpha sub-units (Figure 6). Earlier start codons are predicted to result in non-sense
385 and early stop codons.

386 The 5' end of the urease coding region was targeted to induce a frame shift and disrupt the protein
387 early on, however it may be better to target the active site or entirely remove the gene. Precise
388 deletions larger than a gene using CRISPR-Cas and two sgRNAs have been previously demonstrated
389 [43].

390 **Conclusions**

391 CRISPR-Cas can precisely and efficiently edit the genome of the diatom *Thalassiosira pseudonana*.
392 Twelve percent of initial colonies and 100% which screened positive for Cas9 showed evidence of a
393 mutation in the urease gene, with many sub-clones showing precise bi-allelic 37nt deletions from
394 two sgRNA DSBs. Screening for the deletion by PCR allowed efficient identification of bi-allelic
395 mutants and Golden Gate cloning allowed easy assembly of a plasmid for CRISPR-Cas. This included
396 adapting the system for *T. pseudonana* by including endogenous promoters and two specific sgRNAs.
397 Due to the flexible modular nature of the cloning system, this can be easily adapted for other genes
398 in *T. pseudonana*. A variety of available online tools were used to design two sgRNAs that would
399 target the early coding region of the urease gene. A reduced growth rate and cell-size phenotype
400 was seen in mutant cell-lines grown in urea compared to nitrate, suggesting that function of the
401 urease may have been impaired rather than removed or an alternative source of nitrogen was
402 available.
403 As potentially the most important tool in gene editing to date, CRISPR-Cas is fast becoming a key
404 method in the molecular toolbox for a large variety of organisms. This efficient method has huge
405 potential for future work from both an ecological and biotechnology perspective in *T. pseudonana*
406 and can potentially be easily adapted for many other algal species.

407 **Acknowledgements**

408 This work has been funded by a PhD studentship from the Natural Environment Research Council
409 (NERC) awarded to AH. TM was partially supported by NERC (NE/K013734/1) and the School of
410 Environmental Sciences at UEA. We are thankful to Lewis Dunham for his contributions to the 5'
411 RACE for identifying the U6 promoter.

412

413 **References**

- 414 1. Kooistra WHCF, Medlin LK: **Evolution of the Diatoms (Bacillariophyta)**. *Mol Phylogenet Evol* 1996,
415 **6**:391–407.
- 416 2. Armbrust, E Virginia and Berges, John A and Bowler, Chris and Green, Beverley R and Martinez,
417 Diego and Putnam, Nicholas H and Zhou, Shiguo and Allen, Andrew E and Apt, Kirk E and Bechner M
418 and others: **Lawrence Berkeley National Laboratory Lawrence Berkeley National Laboratory**. 2004.
- 419 3. Bowler C, Allen AE, Badger JH, Grimwood J, Jabbari K, Kuo A, Maheswari U, Martens C, Maumus F,
420 Otiillar RP, Rayko E, Salamov A, Vandepoele K, Beszteri B, Gruber A, Heijde M, Katinka M, Mock T,
421 Valentin K, Verret F, Berges J a, Brownlee C, Cadoret J-P, Chiovitti A, Choi CJ, Coesel S, De Martino A,
422 Detter JC, Durkin C, Falciatore A, et al.: **The Phaeodactylum genome reveals the evolutionary**
423 **history of diatom genomes**. *Nature* 2008, **456**:239–244.
- 424 4. Smetacek V: **Diatoms and the ocean carbon cycle**. *Protist News* 1999, **150**:25–32.
- 425 5. Field CB: **Primary Production of the Biosphere: Integrating Terrestrial and Oceanic Components**.
426 *Science (80-)* 1998, **281**:237–240.
- 427 6. Falkowski PG, Raven JA: *Aquatic Photosynthesis*. Second. Princeton University Press; 2007.

- 428 7. Dolatabadi JEN, de la Guardia M: **Applications of diatoms and silica nanotechnology in**
429 **biosensing, drug and gene delivery, and formation of complex metal nanostructures.** *TrAC - Trends*
430 *Anal Chem* 2011, **30**:1538–1548.
- 431 8. Delalat B, Sheppard VC, Rasi Ghaemi S, Rao S, Prestidge C a., McPhee G, Rogers M-L, Donoghue JF,
432 Pillay V, Johns TG, Kröger N, Voelcker NH: **Targeted drug delivery using genetically engineered**
433 **diatom biosilica.** *Nat Commun* 2015, **6**:8791.
- 434 9. d'Ippolito G, Sardo A, Paris D, Vella FM, Adelfi MG, Botte P, Gallo C, Fontana A: **Potential of lipid**
435 **metabolism in marine diatoms for biofuel production.** *Biotechnol Biofuels* 2015, **8**:28.
- 436 10. Jeffryes C, Campbell J, Li H, Jiao J, Rorrer G: **The potential of diatom nanobiotechnology for**
437 **applications in solar cells, batteries, and electroluminescent devices.** *Energy Environ Sci* 2011,
438 **4**:3930.
- 439 11. Kuczynska P, Jemiola-Rzeminska M, Strzalka K: **Photosynthetic pigments in diatoms.** *Mar Drugs*
440 2015, **13**:5847–5881.
- 441 12. Lander ES: **The Heroes of CRISPR.** *Cell* 2016, **164**:18–28.
- 442 13. Sander JD, Joung JK: **CRISPR-Cas systems for editing, regulating and targeting genomes.** *Nat*
443 *Biotechnol* 2014, **32**:347–55.
- 444 14. Doudna J a., Charpentier E: **The new frontier of genome engineering with CRISPR-Cas9.** *Science*
445 (80-) 2014, **346**:1258096–1258096.
- 446 15. Nymark M, Sharma AK, Sparstad T, Bones AM, Winge P: **A CRISPR/Cas9 system adapted for gene**
447 **editing in marine algae.** *Sci Rep* 2016, **6**(April):24951.
- 448 16. Shin S-E, Lim J-M, Koh HG, Kim EK, Kang NK, Jeon S, Kwon S, Shin W-S, Lee B, Hwangbo K, Kim J,
449 Ye SH, Yun J-Y, Seo H, Oh H-M, Kim K-J, Kim J-S, Jeong W-J, Chang YK, Jeong B: **CRISPR/Cas9-induced**
450 **knockout and knock-in mutations in Chlamydomonas reinhardtii.** *Sci Rep* 2016, **6**(April):27810.
- 451 17. Weyman PD, Beeri K, Lefebvre SC, Rivera J, Mccarthy JK, Heuberger AL, Peers G, Allen AE, Dupont
452 CL: **Inactivation of Phaeodactylum tricornutum urease gene using transcription activator-like**
453 **effector nuclease-based targeted mutagenesis.** *Plant Biotechnol J* 2015, **13**:460–470.
- 454 18. Daboussi F, Leduc S, Maréchal A, Dubois G, Guyot V, Perez-Michaut C, Amato A, Falciatore A,
455 Juillerat A, Beurdeley M, Voytas DF, Cavarec L, Duchateau P: **Genome engineering empowers the**
456 **diatom Phaeodactylum tricornutum for biotechnology.** *Nat Commun* 2014, **5**(May):3831.
- 457 19. Poulsen N, Chesley PM, Kröger N: **Molecular genetic manipulation of the diatom Thalassiosira**
458 **pseudonana (Bacillariophyceae).** *J Phycol* 2006, **42**:1059–1065.
- 459 20. Karas BJ, Diner RE, Lefebvre SC, McQuaid J, Phillips APR, Noddings CM, Brunson JK, Valas RE,
460 Deerinck TJ, Jablanovic J, Gillard JTF, Beeri K, Ellisman MH, Glass JI, Hutchison III C a., Smith HO,
461 Venter JC, Allen AE, Dupont CL, Weyman PD: **Designer diatom episomes delivered by bacterial**
462 **conjugation.** *Nat Commun* 2015, **6**:6925.
- 463 21. Cook O, Hildebrand M: **Enhancing LC-PUFA production in Thalassiosira pseudonana by**
464 **overexpressing the endogenous fatty acid elongase genes.** *J Appl Phycol* 2015, **28**:897–905.

- 465 22. Doan TTY, Sivaloganathan B, Obbard JP: **Screening of marine microalgae for biodiesel feedstock.**
466 *Biomass and Bioenergy* 2011, **35**:2534–2544.
- 467 23. Malviya S, Scalco E, Audic S, Vincent F, Veluchamy A, Bittner L, Poulain J, Wincker P, Iudicone D,
468 de Vargas C, Zingone A, Bowler C: **Insights into global diatom distribution and diversity in the**
469 **world's ocean.** *Proc Natl Acad Sci* 2015, **348**:in review.
- 470 24. Shrestha RP, Hildebrand M: **Evidence for a regulatory role of diatom silicon transporters in**
471 **cellular silicon responses.** *Eukaryot Cell* 2015, **14**:29.
- 472 25. Scheffel A, Poulsen N, Shian S, Kröger N: **Nanopatterned protein microrings from a diatom that**
473 **direct silica morphogenesis.** *Proc Natl Acad Sci U S A* 2011, **108**:3175–3180.
- 474 26. Poulsen N, Scheffel A, Sheppard VC, Chesley PM, Kröger N: **Pentalysine clusters mediate silica**
475 **targeting of silaffins in *Thalassiosira pseudonana*.** *J Biol Chem* 2013, **288**:20100–20109.
- 476 27. Xing H-L, Dong L, Wang Z-P, Zhang H-Y, Han C-Y, Liu B, Wang X-C, Chen Q-J: **A CRISPR/Cas9**
477 **toolkit for multiplex genome editing in plants.** *BMC Plant Biol* 2014, **14**:327.
- 478 28. Weber E, Engler C, Gruetzner R, Werner S, Marillonnet S: **A modular cloning system for**
479 **standardized assembly of multigene constructs.** *PLoS One* 2011, **6**.
- 480 29. Doench JG, Hartenian E, Graham DB, Tothova Z, Hegde M, Smith I, Sullender M, Ebert BL, Xavier
481 RJ, Root DE: **Rational design of highly active sgRNAs for CRISPR-Cas9-mediated gene inactivation.**
482 *Nat Biotechnol* 2014, **32**:1262–7.
- 483 30. Xiao A, Cheng Z, Kong L, Zhu Z, Lin S, Gao G, Zhang B: **CasOT: A genome-wide Cas9/gRNA off-**
484 **target searching tool.** *Bioinformatics* 2014, **30**:1180–1182.
- 485 31. Tarleton R, Peng D: **EuPaGDT: a web tool tailored to design CRISPR guide RNAs for eukaryotic**
486 **pathogens.** *Microb Genomics* 2015, **1**:1–7.
- 487 32. Nekrasov V, Staskawicz B, Weigel D, Jones JDG, Kamoun S: **Targeted mutagenesis in the model**
488 **plant *Nicotiana benthamiana* using Cas9 RNA-guided endonuclease.** *Nat Biotechnol* 2013, **31**:691–
489 693.
- 490 33. Belhaj K, Chaparro-Garcia A, Kamoun S, Nekrasov V: **Plant genome editing made easy: targeted**
491 **mutagenesis in model and crop plants using the CRISPR/Cas system.** *Plant Methods* 2013, **9**:39.
- 492 34. Price, N.M., Harrison, G.I., Hering, J.G., Hudson, R.J., Nirel, P.M., Palenik, B. and Morel FM:
493 **Preparation and Chemistry of the Artificial Algal Culture Medium Aquil.** *Biol Oceanogr* 1989, **6**:443–
494 461.
- 495 35. Pinto FL, Lindblad P: **A guide for in-house design of template-switch-based 5'?? rapid**
496 **amplification of cDNA ends systems.** *Anal Biochem* 2010, **397**:227–232.
- 497 36. Stothard P: **The Sequence Manipulation Suite: JavaScript Programs for Analyzing and**
498 **Formatting Protein and DNA Sequences.** *Biotechniques* 2000, **28**:1102–1104.

- 499 37. Brooks, C., Nekrasov, V., Lippman, Z.B. and Van Eck J: **Efficient Gene Editing in Tomato in the**
500 **First Generation Using the Clustered Regularly Interspaced Short Palindromic Repeats/CRISPR-**
501 **Associated9 System1.** *Plant Physiol* 2014, **166**:1292–1297.
- 502 38. Jacobs TB, LaFayette PR, Schmitz RJ, Parrott W a: **Targeted genome modifications in soybean**
503 **with CRISPR/Cas9.** *BMC Biotechnol* 2015, **15**:16.
- 504 39. Sakuma T, Nishikawa A, Kume S, Chayama K, Yamamoto T: **Multiplex genome engineering in**
505 **human cells using all-in-one CRISPR/Cas9 vector system.** *Sci Rep* 2014, **4**:5400.
- 506 40. Port F, Chen H-M, Lee T, Bullock SL: **Optimized CRISPR/Cas tools for efficient germline and**
507 **somatic genome engineering in *Drosophila*.** *Proc Natl Acad Sci U S A* 2014, **111**:E2967–2976.
- 508 41. Weber E, Gruetzner R, Werner S, Engler C, Marillonnet S: **Assembly of designer tal effectors by**
509 **golden gate cloning.** *PLoS One* 2011, **6**.
- 510 42. Krysiak C, Mazus B, Buchowicz J: **Relaxation, linearization and fragmentation of supercoiled**
511 **circular DNA by tungsten microprojectiles.** *Transgenic Res* 1999, **8**:303–306.
- 512 43. Zheng Q, Cai X, Tan MH, Schaffert S, Arnold CP, Gong X, Chen CZ, Huang S: **Precise gene deletion**
513 **and replacement using the CRISPR/Cas9 system in human cells.** *Biotechniques* 2014, **57**:115–124.
- 514 44. Jinek M, Chylinski K, Fonfara I, Hauer M, Doudna J a, Charpentier E: **A Programmable Dual-RNA –**
515 **Guided.** 2012, **337**(August):816–822.
- 516 45. Gupta S, Kathait A, Sharma V: **Computational Sequence Analysis and Structure Prediction of**
517 **Jack Bean Urease.** 2015, **3**:185–191.
- 518 46. Olson RJ, Vaultot D, Chisholm SW: **Effects of environmental stresses on the cell cycle of 2 marine**
519 **phytoplankton species.** *Plant Physiol* 1986, **80**:918–925.
- 520 47. Li W, Gao K, Beardall J: **Interactive Effects of Ocean Acidification and Nitrogen-Limitation on the**
521 **Diatom *Phaeodactylum tricornutum*.** *PLoS One* 2012, **7**.
- 522 48. Fan C, Glibert PM, Alexander J, Lomas MW: **Characterization of urease activity in three marine**
523 **phytoplankton species, *Aureococcus anophagefferens*, *Prorocentrum minimum*, and *Thalassiosira***
524 ***weissflogii*.** *Mar Biol* 2003, **142**:949–958.
- 525 49. Habel JE, Bursey EH, Rho BS, Kim CY, Segelke BW, Rupp B, Park MS, Terwilliger TC, Hung LW:
526 **Structure of Rv1848 (UreA), the *Mycobacterium tuberculosis* urease ?? subunit.** *Acta Crystallogr*
527 *Sect F Struct Biol Cryst Commun* 2010, **66**:781–786.
- 528 50. Jabri E, Andrew Karplus P: **Structures of the *Klebsiella aerogenes* urease apoenzyme and two**
529 **active- site mutants.** *Biochemistry* 1996, **35**:10616–10626.
- 530 51. Hellen CUT, Sarnow P: **Internal ribosome entry sites in eukaryotic mRNA molecules Internal**
531 **ribosome entry sites in eukaryotic mRNA molecules.** 2001:1593–1612.

532

533 **Figure captions**

534 **Table 1.** Oligonucleotides used in this study. Ref. N^o 1-3: oligos used in 5' RACE [35]. Ref. N^o 4-16:
535 primers for Golden Gate cloning, BsaI sites are underlined, 4nt overhangs are shown in *italics*, and
536 sgRNA targets are shown in **bold**. Upper case indicates complement to the template. Ref. N^o 17-20:
537 primers for SDM, lower case indicates base change. Ref. N^o 21-26: primers for screening
538 transformants. Ref. N^o 27-35: primers for sequencing the CRISPR-Cas construct.

539 **Figure 1.** Overview of level 1 and level 2 Golden Gate cloning for assembly of the CRISPR-Cas
540 construct pAGM4723:TpCC_Urease. Level 1 assemblies of pICH47742:FCP:Cas9YFP and
541 pICH47751:U6:sgRNA_Urease 1 are shown. BsaI or BpiI restriction enzymes cut outside the
542 recognition site leading to specific 4nt overhangs which are complementary to adjacent modules,
543 allowing several modules to be accurately assembled in one reaction. Complementary 4nt
544 sequences are colour coded to indicate adjacent modules.

545 **Figure 2.** Screening by PCR and sequencing. Expected sgRNA cut indicated by ↓. PCR of targeted
546 urease fragments from primary clones show a single higher MW band for M1 and WT, a lower MW
547 band associated with the expected 37nt deletion for M4 and LM1 and two bands for M2 & M3.
548 Sequence alignments of urease products with mutations are shown for primary clones. A few
549 examples of PCR products from sub-clones are shown. Primary clones M2 and M3 appear to be
550 mosaic with sub-clones containing bi-allelic and mixed products corresponding to full length urease
551 and the lower MW band associated with the deletion. Sequence alignments from mono-allelic sub-
552 clone M1_9 and bi-allelic sub-clones from M2 and M3 are shown.

553 **Figure 3.** Growth rate of WT and mutant urease cell lines from two separate growth experiments (1)
554 & (2). The WT cell line was grown in nitrate free (white), nitrate (dark grey) and urea (light grey)
555 enriched media. Mutant cell lines were grown in nitrate or urea enriched media. Growth rate
556 (division day⁻¹) was measured in exponential phase and rates compared using analysis of variance
557 with Tukey's pairwise comparisons.

558 **Figure 4.** Mean cell size (μm) measured at the end of exponential phase for WT and mutant cultures
559 across two growth experiments (1) & (2). Cells were grown with nitrate (dark grey) or urea (light
560 grey) as the sole nitrogen source. Cell size was compared using analysis of variance with Tukey's
561 pairwise comparisons.

562 **Figure 5.** PCR of the targeted urease fragment following growth of WT and mutant cell lines in
563 nitrate or urea. NEB 100bp ladder (1), WT in nitrate (2) and urea (3), M2_10 in nitrate (4) and urea
564 (5) and M3_9 in nitrate (6) and urea (7).

565 **Figure 6.** Translated WT urease (a), frame 3 (b) and frame 1 of urease with the expected 37nt
566 deletion (c) and frame 1 of urease with a 38nt deletion (d). Position of deletion indicated by ↓. The
567 model WT protein contains 807aa. The figure shows the initial 260 amino acids for a and c including
568 the start of the alpha sub-unit. Translations are identical for the unshown segments. Gamma (pink),
569 Beta (green) and Alpha (blue) sub-units are highlighted in order. Expected start codon (red) and
570 upstream out-of-frame start codons (grey) are highlighted.

571 **Supplementary Figure 1.** Screenshot of the final spreadsheet for choosing sgRNAs.

Name	Sequence	Ref. No
GS U6 R	AGGTTTGCTTCTCTTCGATTATG	1
TSO	GTCGCACGGTCCATCGCAGCAGTCACAGGGGG	2
U sense	GTCGCACGGTCCATCGCAGCAGTC	3
Fcp:Nat F	<u>tggtctcaggag</u> CTCGAGGTCGACGGTATC	4
Fcp:Nat R	<u>aggtctcaagcg</u> CGCAATTAACCCTCACTAAAGG	5
FCP prom F	<u>tggtctcaggag</u> AGCTTGCGCTTTTCCGAG	6
FCP prom R	<u>aggtctca</u> catTTTGGTATTGGTTTGGTAAATCAG	7
Cas9:YFP F	<u>aggtctca</u> aATGGACAAGAAGTACTCCATTGG	8
Cas9:YFP R	<u>aggtctca</u> aagcTCACTTGTACAGCTCGTCCATG	9
FCP term F	<u>aggtctcagctt</u> ATACTGGATTGGTGAATCAATG	10
FCP term R	<u>tggtctcaagcg</u> GAGAACTGGAGCAGCTAC	11
U6 prom F	<u>cggctcaggag</u> CTTCATCAAGAGAGCAACCA	12
U6 prom R	<u>aggtctca</u> ACAATTTTCGGCAAACCGT	13
Urease sgRNA1 F	<u>aggtctcattgtgtcgtaatcaagtattgccg</u> GTTTTAGAGCTAGAAATAGCAAG	14
Urease sgRNA2 F	<u>aggtctcattgtgttccgatctaatgtccat</u> GTTTTAGAGCTAGAAATAGCAAG	15
Urease sgRNA R	<u>tggtctcaagcg</u> TAATGCCAACTTTGTACAAG	16
FCP prom SDM F	TCCGCGGCAGaTCTCTGTCG	17
FCP prim SDM R	AGAAGTACCGTGTGTTGTCAGTG	18
NAT SDM F	CGACACCGTaTTCCGCGTCAC	19
NAT SDM R	GTGGTGAAGGACCCATCCAG	20
Cas9 screen F	CCGAGACAAGCAGAGTGGAAG	21
Cas9 screen R	AGAGCCGATTGATGTCCAGTTC	22
NAT screen F	ATGACCACTCTTGACGACAC	23
NAT screen R	TTGATTCACCAATCCAGTATGC	24
Urease screen F 1	AAACAGACCACCTTCACCTC	25
Urease screen R	CTCCACCTGTACGTCTCG	26
Fcp seq F	CCATAAGTCAACGGCTCCAATC	27
NAT seq F	CTCTTGACGACACGGCTTAC	28
Cas9 seq 1 F	CATTACGGACGAGTACAAGGTG	29
Cas9 seq 2 F	TGAACACGGAGATCACCAAAG	30
Cas9 seq 3 F	CTTCTTGACAATGAGGAGAAC	31
Cas9 seq 4 F	CAAACCTGATCACACAACGGAAG	32
YFP FcpT seq F	ACTACCTGAGCTACCAGTCC	33
sg2 seq R	GTTTCCGATCTAATGTCCAT	34
sg1 seq F	TGTGTCGTAATCAAGTATTGC	35

Table 1

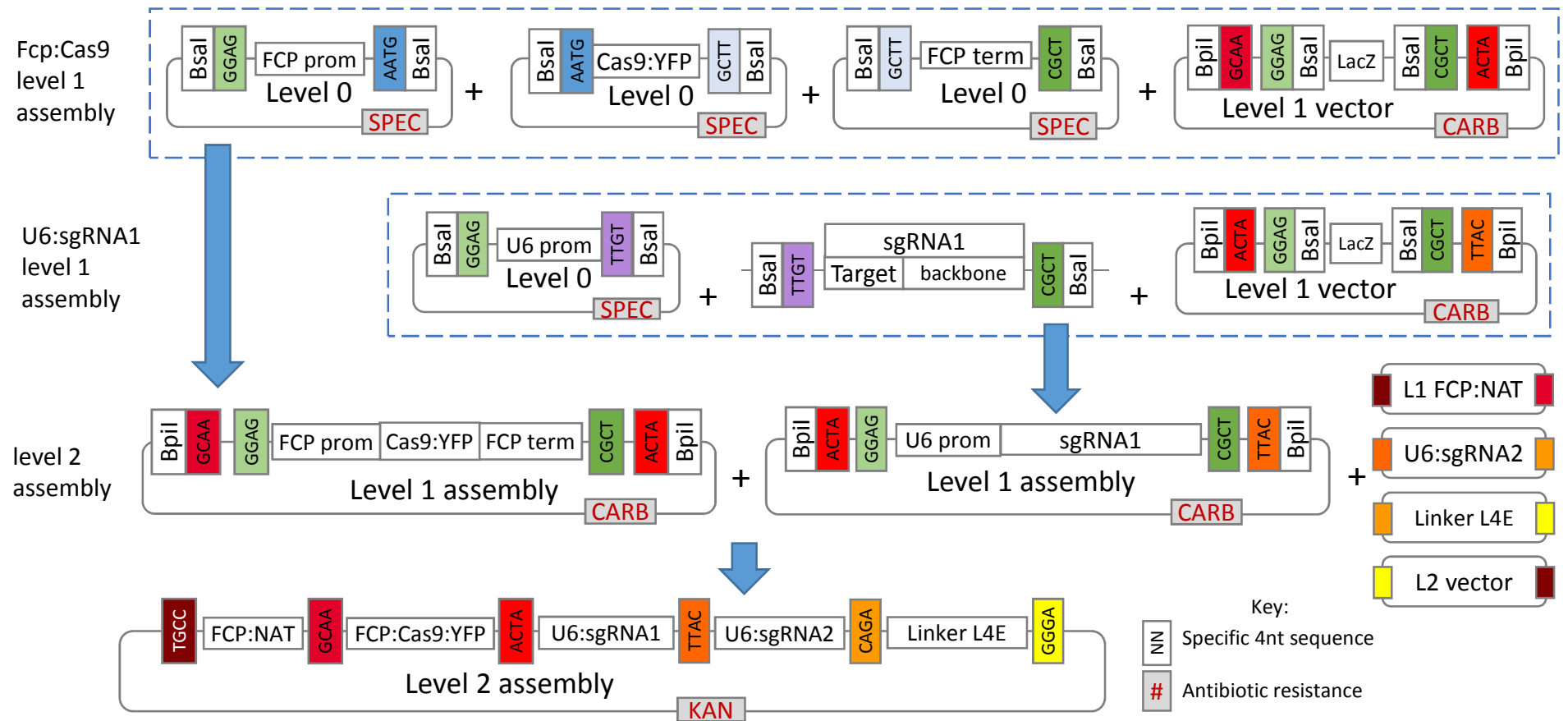
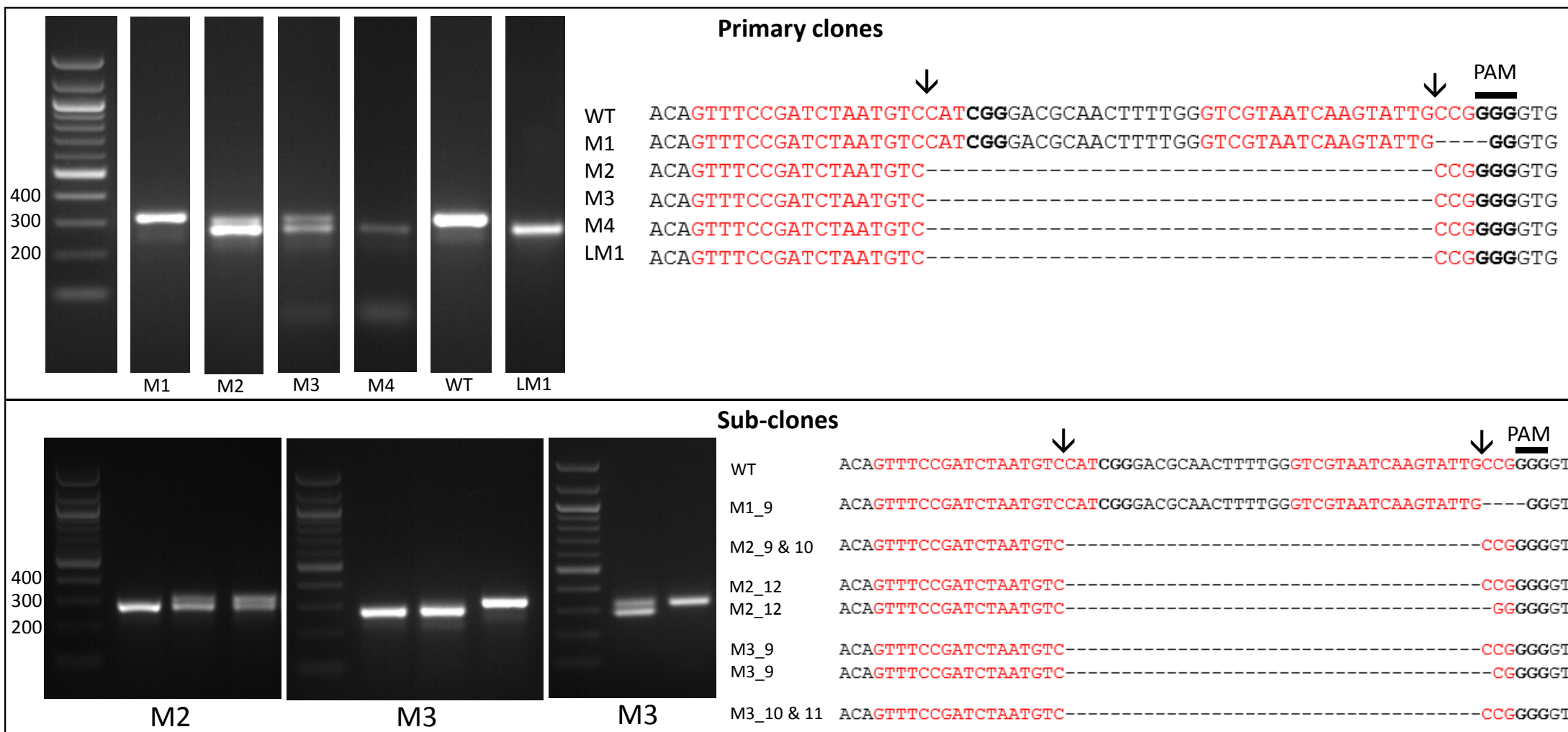


Figure 1



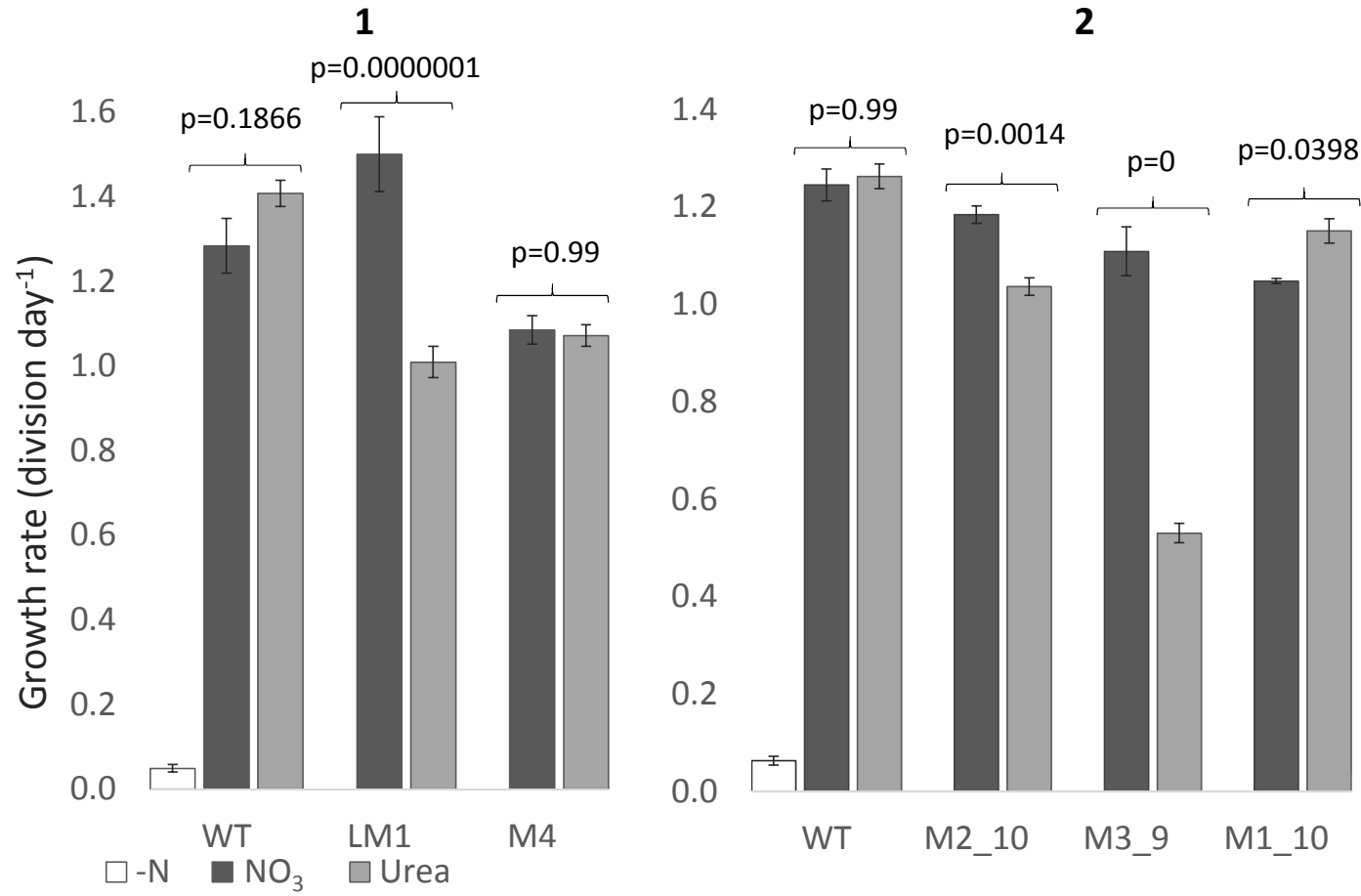


Figure 3

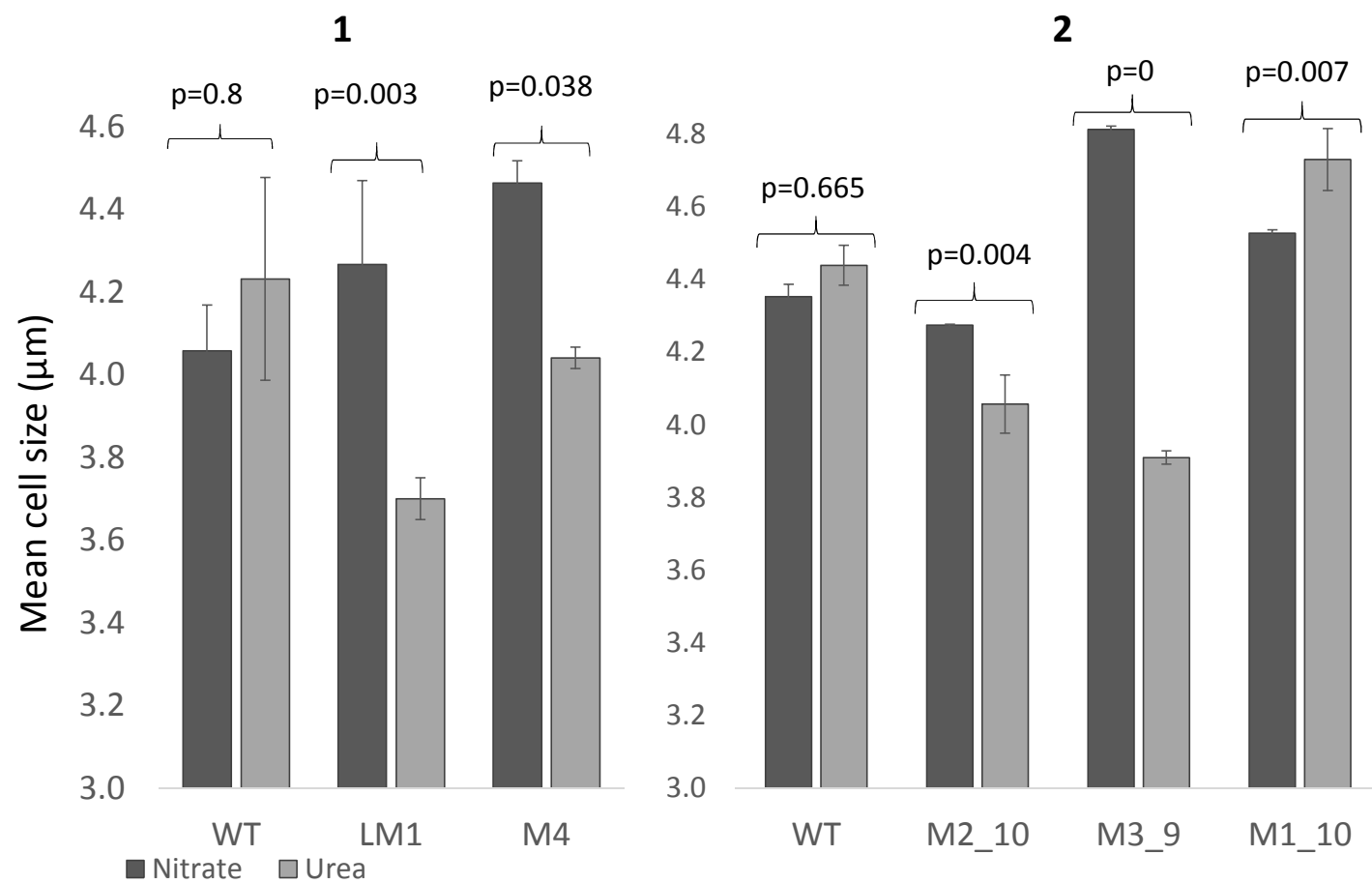


Figure 4

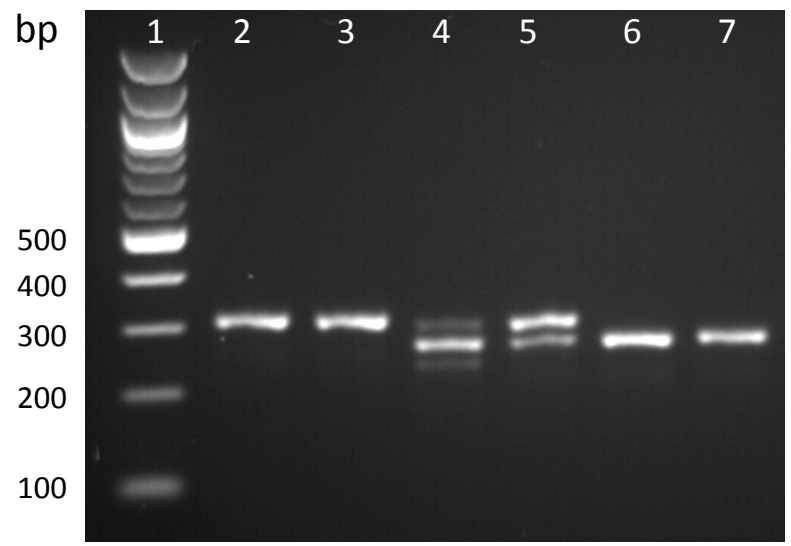


Figure 5

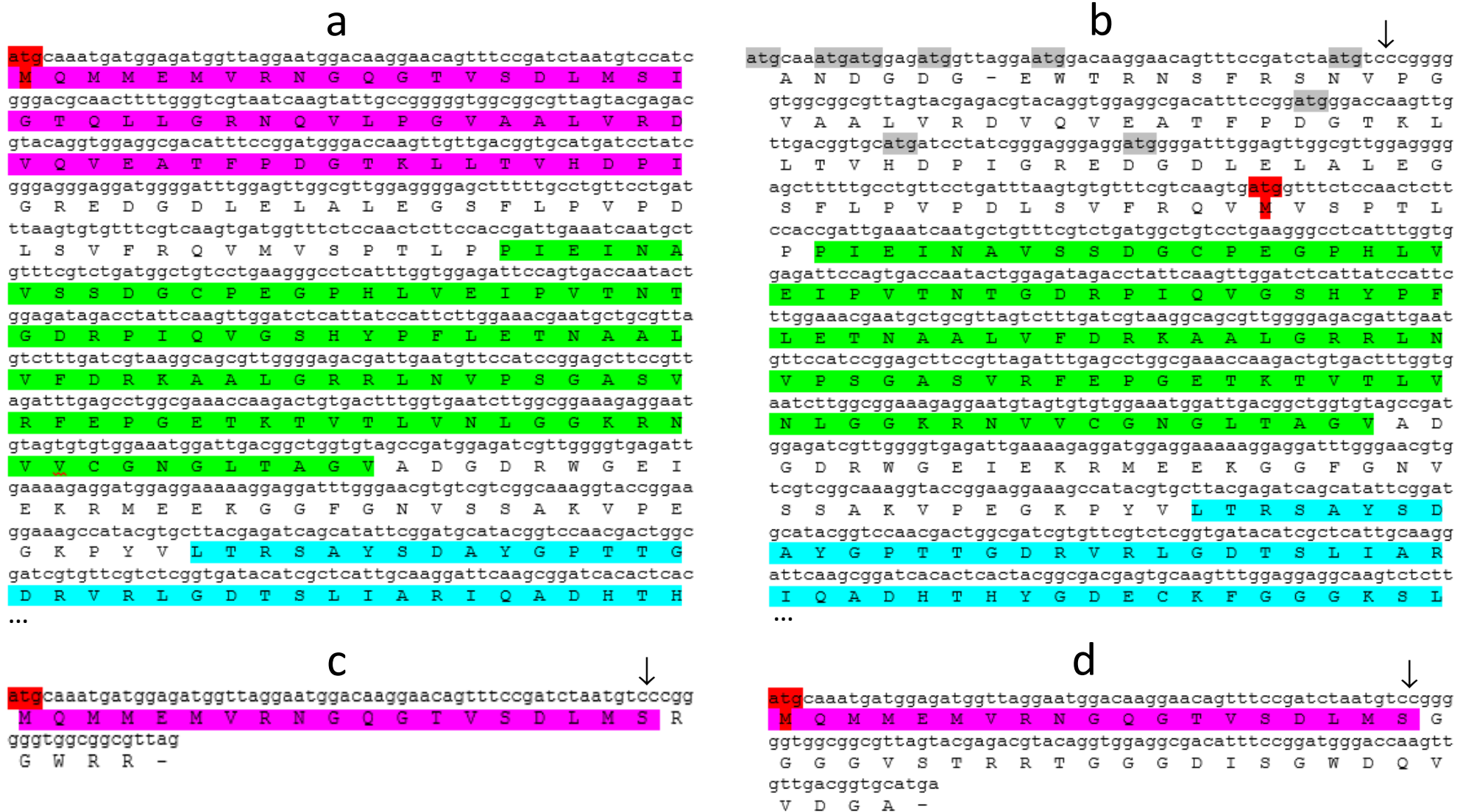


Figure 6

Target sequence	bp No	Cas9 cut	GC	5'	PAM	Location	Strand	Sense sequence	sgRNA score	Restriction sites
GCCTCGAGTAGAAGTCACCG	41	44	40%	G	TGG	Intron1	-	CGGTGACTTCTACTCGAGGC	0.8898	HphI
GCTCATTGCAAGGATTCAAG	915	932	45%	G	CGG	Exon3	+	GCTCATTGCAAGGATTCAAG	0.8388	
GTCGTAATCAAGTATTGCCG	158	175	40%	G	GGG	Exon2	+	GTCGTAATCAAGTATTGCCG	0.7908	HpaII
GTTGGGGTGAGATTGAAAAG	755	772	40%	G	AGG	Exon3	+	GTTGGGGTGAGATTGAAAAG	0.7898	
GACTATTCATGCTTACCACA	1659	1676	55%	G	CGG	Exon3	+	GACTATTCATGCTTACCACA	0.7731	
GCATCATTTCCACATGACCA	1380	1383	30%	G	GGG	Exon3	-	TGGTCATGTGGAAATGATGC	0.6920	
GTGACTTTGGTGAATCTTGG	676	693	35%	G	CGG	Exon3	+	GTGACTTTGGTGAATCTTGG	0.6834	
GTAGCCGATGGAGATCGTTG	739	756	60%	G	GGG	Exon3	+	GTAGCCGATGGAGATCGTTG	0.6533	
GATTTAAGTGTGTTTCGTGG	319	336	45%	G	TGG	Exon2	+	GATTTAAGTGTGTTTCGTGG	0.6478	
GGATGGGACCAAGTTGTTGA	225	242	45%	G	CGG	Exon2	+	GGATGGGACCAAGTTGTTGA	0.5997	
GAGAGGTCATCACTCGTACG	2048	2065	35%	G	TGG	Exon4	+	GAGAGGTCATCACTCGTACG	0.5634	Maell Csp6I SplI
GGAGTCACTACAATGTTTGG	1306	1323	40%	G	AGG	Exon3	+	GGAGTCACTACAATGTTTGG	0.5336	
GGTGCATGATCCTATCGGGA	246	263	65%	G	GGG	Exon2	+	GGTGCATGATCCTATCGGGA	0.5331	
GGTAATCCGGATAACAATGAA	1138	1155	50%	G	TGG	Exon3	+	GGTAATCCGGATAACAATGAA	0.5016	TspDI
GTTTCCGATCTAATGTCCAT	121	138	55%	G	CGG	Exon2	+	GTTTCCGATCTAATGTCCAT	0.5004	BclI
GAATGGATGGATCAAGGTGG	1905	1908	55%	G	TGG	Exon4	-	CCACCTTGATCCATCCATTC	0.4847	
GATTGTACCAGGTCAAGTGA	411	428	40%	G	TGG	Intron2	+	GATTGTACCAGGTCAAGTGA	0.4808	
GGAGATAGACCTATTCAAGT	529	546	50%	G	TGG	Exon3	+	GGAGATAGACCTATTCAAGT	0.4788	
GCAACTACTGATGTAATTGC	1198	1215	50%	G	GGG	Exon3	+	GCAACTACTGATGTAATTGC	0.4781	MluCI
GATGGTATCGGAGAACGATT	2467	2484	45%	G	GGG	Exon4	+	GATGGTATCGGAGAACGATT	0.4765	
GCGATAGCGTGGGCTCAGAT	2317	2334	50%	G	GGG	Exon4	+	GCGATAGCGTGGGCTCAGAT	0.4762	BclI BseMII
GTGGAGGCGACATTTCCGGA	208	225	40%	G	TGG	Exon2	+	GTGGAGGCGACATTTCCGGA	0.4649	BseGI HpaII BspMII

Supplementary Figure 1